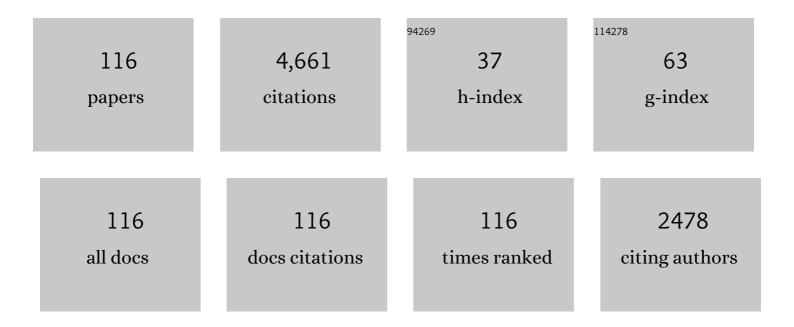
## Haibo Zhang

List of Publications by Year in descending order

Source: https://exaly.com/author-pdf/5050134/publications.pdf Version: 2024-02-01



ΗΛΙΒΟ ΖΗΛΝΟ

#	Article	IF	CITATIONS
1	Enhanced energy-storage performance with excellent stability under low electric fields in BNT–ST relaxor ferroelectric ceramics. Journal of Materials Chemistry C, 2019, 7, 281-288.	2.7	324
2	Preparation and enhanced electrical properties of grain-oriented (Bi1/2Na1/2)TiO3-based lead-free incipient piezoceramics. Journal of the European Ceramic Society, 2015, 35, 2501-2512.	2.8	219
3	A review on the development of lead-free ferroelectric energy-storage ceramics and multilayer capacitors. Journal of Materials Chemistry C, 2020, 8, 16648-16667.	2.7	184
4	Ultrahigh dielectric breakdown strength and excellent energy storage performance in lead-free barium titanate-based relaxor ferroelectric ceramics via a combined strategy of composition modification, viscous polymer processing, and liquid-phase sintering. Chemical Engineering Journal, 2020, 398, 125625.	6.6	181
5	Enhanced energy density of polymer nanocomposites at a low electric field through aligned BaTiO <sub>3</sub> nanowires. Journal of Materials Chemistry A, 2017, 5, 6070-6078.	5.2	175
6	Polymer Matrix Nanocomposites with 1D Ceramic Nanofillers for Energy Storage Capacitor Applications. ACS Applied Materials & amp; Interfaces, 2020, 12, 1-37.	4.0	163
7	Ultrahigh discharged energy density in polymer nanocomposites by designing linear/ferroelectric bilayer heterostructure. Nano Energy, 2018, 54, 437-446.	8.2	137
8	Large Strain in Relaxor/Ferroelectric Composite Leadâ€Free Piezoceramics. Advanced Electronic Materials, 2015, 1, 1500018.	2.6	120
9	Energy storage performance of Na0.5Bi0.5TiO3 based lead-free ferroelectric ceramics prepared via non-uniform phase structure modification and rolling process. Chemical Engineering Journal, 2021, 420, 130475.	6.6	102
10	Advanced Catalysts for Photoelectrochemical Water Splitting. ACS Applied Energy Materials, 2021, 4, 12007-12031.	2.5	94
11	Temperature-insensitive electric-field-induced strain and enhanced piezoelectric properties of <001> textured (K,Na)NbO3-based lead-free piezoceramics. Acta Materialia, 2018, 156, 389-398.	3.8	84
12	Bi1/2Na1/2TiO3–BaTiO3 based thick-film capacitors for high-temperature applications. Journal of the European Ceramic Society, 2014, 34, 37-43.	2.8	82
13	Ultrahigh energy density and thermal stability in sandwich-structured nanocomposites with dopamine@Ag@BaTiO3. Energy Storage Materials, 2020, 31, 492-504.	9.5	80
14	High discharged energy density of polymer nanocomposites containing paraelectric SrTiO3 nanowires for flexible energy storage device. Journal of Alloys and Compounds, 2018, 744, 116-123.	2.8	78
15	Progress and perspective of high strain NBT-based lead-free piezoceramics and multilayer actuators. Journal of Materiomics, 2021, 7, 508-544.	2.8	76
16	Relaxor/antiferroelectric composites: a solution to achieve high energy storage performance in lead-free dielectric ceramics. Journal of Materials Chemistry C, 2020, 8, 5681-5691.	2.7	75
17	Largely enhanced discharge energy density in linear polymer nanocomposites by designing a sandwich structure. Composites Part A: Applied Science and Manufacturing, 2019, 121, 115-122.	3.8	73
18	Novel NaNbO3–Sr0.7Bi0·2TiO3 lead-free dielectric ceramics with excellent energy storage properties. Ceramics International, 2021, 47, 3713-3719.	2.3	70

#	Article	IF	CITATIONS
19	Fine-grained BNT-based lead-free composite ceramics with high energy-storage density. Ceramics International, 2019, 45, 19895-19901.	2.3	68
20	Large electric field-induced strain in AgNbO3-modified 0.76Bi0.5Na0.5TiO3-0.24SrTiO3 lead-free piezoceramics. Ceramics International, 2018, 44, 7851-7857.	2.3	66
21	Droplet impact on soft viscoelastic surfaces. Physical Review E, 2016, 94, 063117.	0.8	65
22	Tailoring the energy storage performance of polymer nanocomposites with aspect ratio optimized 1D nanofillers. Journal of Materials Chemistry A, 2018, 6, 20356-20364.	5.2	63
23	Effects of CoFe 2 O 4 electrode microstructure on the sensing properties for mixed potential NH 3 sensor. Sensors and Actuators B: Chemical, 2017, 239, 462-466.	4.0	61
24	Large strain with low hysteresis in Bi4Ti3O12 modified Bi1/2(Na0.82K0.18)1/2TiO3 lead-free piezoceramics. Journal of the European Ceramic Society, 2018, 38, 4404-4413.	2.8	61
25	High Energy Storage Performance of PMMA Nanocomposites Utilizing Hierarchically Structured Nanowires Based on Interface Engineering. ACS Applied Materials & Interfaces, 2021, 13, 27382-27391.	4.0	59
26	Superior energy-storage performance in 0.85Bi <sub>0.5</sub> Na <sub>0.5</sub> TiO <sub>3</sub> –0.15NaNbO <sub>3</sub> lead-free ferroelectric ceramics <i>via</i> composition and microstructure engineering. Journal of Materials Chemistry A, 2021, 9, 10088-10094.	5.2	57
27	Constructing layered structures to enhance the breakdown strength and energy density of Na <sub>0.5</sub> Bi <sub>0.5</sub> TiO <sub>3</sub> -based lead-free dielectric ceramics. Journal of Materials Chemistry C, 2019, 7, 15292-15300.	2.7	51
28	High energy density at high temperature in PLZST antiferroelectric ceramics. Journal of Materials Chemistry C, 2019, 7, 4587-4594.	2.7	49
29	Effect of V 2 O 5 -content on electrode catalytic layer morphology and mixed potential ammonia sensor performance. Sensors and Actuators B: Chemical, 2016, 223, 658-663.	4.0	47
30	Improved heat transfer for pyroelectric energy harvesting applications using a thermal conductive network of aluminum nitride in PMN–PMS–PZT ceramics. Journal of Materials Chemistry A, 2018, 6, 5040-5051.	5.2	45
31	Largely enhanced ferroelectric and energy storage performances of P(VDF-CTFE) nanocomposites at a lower electric field using BaTiO3 nanowires by stirring hydrothermal method. Ceramics International, 2016, 42, 19012-19018.	2.3	43
32	Large electric-field-induced strain in B-site complex-ion (Fe0.5Nb0.5)4+-doped Bi1/2 (Na0.82K0.12)1/2TiO3 lead-free piezoceramics. Ceramics International, 2018, 44, 3211-3217.	2.3	43
33	Waste biomass valorization through production of xylose-based porous carbon microspheres for supercapacitor applications. Waste Management, 2020, 105, 492-500.	3.7	41
34	Hydrothermal Synthesis and Sizeâ€Dependent Properties of Multiferroic Bismuth Ferrite Crystallites. Journal of the American Ceramic Society, 2010, 93, 3842-3849.	1.9	39
35	Thermally-stable large strain in Bi(Mn0.5Ti0.5)O3 modified 0.8Bi0.5Na0.5TiO3-0.2Bi0.5K0.5TiO3 ceramics. Journal of the European Ceramic Society, 2019, 39, 1827-1836.	2.8	39
36	Large strain under low driving field in leadâ€free relaxor/ferroelectric composite ceramics. Journal of the American Ceramic Society, 2019, 102, 4113-4126.	1.9	39

#	Article	IF	CITATIONS
37	Phase evolution and relaxor to ferroelectric phase transition boosting ultrahigh electrostrains in (1â^'x)(Bi1/2Na1/2)TiO3-x(Bi1/2K1/2)TiO3 solid solutions. Journal of Materiomics, 2022, 8, 335-346.	2.8	39
38	Sandwich structure-assisted significantly improved discharge energy density in linear polymer nanocomposites with high thermal stability. Colloids and Surfaces A: Physicochemical and Engineering Aspects, 2019, 581, 123802.	2.3	38
39	Review of lead-free Bi-based dielectric ceramics for energy-storage applications. Journal Physics D: Applied Physics, 2021, 54, 293001.	1.3	38
40	Pyroelectric and Dielectric Properties of Mn Modified 0.82Bi <sub>0.5</sub> Na <sub>0.5</sub> TiO <sub>3</sub> –0.18Bi <sub>0.5</sub> K <sub>0.5</sub> TiO <sub> Leadâ€Free Thick Films. Journal of the American Ceramic Society, 2009, 92, 2147-2150.</sub>	,3 <b>r.</b> ¢sub>	37
41	Highly enhanced thermal stability in quenched Na0.5Bi0.5TiO3-based lead-free piezoceramics. Journal of the European Ceramic Society, 2019, 39, 4705-4711.	2.8	37
42	Structure variation and energy storage properties of acceptorâ€modified <scp>PBLZST</scp> antiferroelectric ceramics. Journal of the American Ceramic Society, 2019, 102, 1912-1920.	1.9	36
43	Large electrostrain in Iowâ€temperature sintered NBTâ€BTâ€0.025FN incipient piezoceramics. Journal of the American Ceramic Society, 2020, 103, 3739-3747.	1.9	36
44	Effects of sintering temperature on sensing properties of V2O5-WO3-TiO2 electrode for potentiometric ammonia sensor. Sensors and Actuators B: Chemical, 2017, 241, 268-275.	4.0	35
45	Hexagonal boron nitride nanosheets doped pyroelectric ceramic composite for high-performance thermal energy harvesting. Nano Energy, 2019, 60, 144-152.	8.2	34
46	Ultrahigh energy storage density of Ca2+-modified PLZST antiferroelectric ceramics prepared by the tape-casting method. Journal of the European Ceramic Society, 2021, 41, 4138-4145.	2.8	33
47	High discharged energy density of nanocomposites filled with double-layered core-shell nanoparticles by reducing space charge polarization. Ceramics International, 2018, 44, 19330-19337.	2.3	31
48	Enhanced Dielectric Energy Storage Performance of 0.45Na <sub>0.5</sub> Bi <sub>0.5</sub> TiO <sub>3</sub> -0.55Sr <sub>0.7</sub> Bi <sub>0.2</sub> TiO <sub>3 0–3 Type Lead-Free Composite Ceramics. ACS Applied Materials &amp; Interfaces, 2022, 14, 17652-17661.</sub>	<b sud>/All	N 31
49	Low temperature preparation and electrical properties of sodium–potassium bismuth titanate lead-free piezoelectric thick films by screen printing. Journal of the European Ceramic Society, 2010, 30, 3157-3165.	2.8	30
50	(Na <sub>1/2</sub> Bi <sub>1/2</sub> )TiO <sub>3</sub> â€based leadâ€free coâ€fired multilayer actuators with large strain and high fatigue resistance. Journal of the American Ceramic Society, 2019, 102, 6147-6155.	1.9	30
51	Achieving excellent energy storage density of Pb0.97La0.02(Zr Sn0.05Ti0.95-)O3 ceramics by the B-site modification. Journal of the European Ceramic Society, 2021, 41, 360-367.	2.8	30
52	Dielectric, Ferroelectric, Pyroelectric, and Piezoelectric Properties of Laâ€Modified Leadâ€Free Sodium–Potassium Bismuth Titanate Thick Films. Journal of the American Ceramic Society, 2010, 93, 750-757.	1.9	29
53	Significant Energy Density of Discharge and Charge–Discharge Efficiency in Ag@BNN Nanofillers-Modified Heterogeneous Sandwich Structure Nanocomposites. ACS Applied Energy Materials, 2020, 3, 6591-6601.	2.5	29
54	Preparation and characterization of sol–gel derived sodium–potassium bismuth titanate powders and thick films deposited by screen printing. Journal of Alloys and Compounds, 2010, 495, 173-180.	2.8	28

#	Article	IF	CITATIONS
55	Piezoelectric property in morphotropic phase boundary Bi0.5(Na0.82K0.18)0.5TiO3 lead free thick film deposited by screen printing. Applied Physics Letters, 2008, 92, 152901.	1.5	27
56	Effect of repeated composite sol infiltrations on the dielectric and piezoelectric properties of a Bi0.5(Na0.82K0.18)0.5TiO3 lead free thick film. Journal of the European Ceramic Society, 2009, 29, 717-723.	2.8	27
57	Effects of sintering temperature on the NH3 sensing properties of Mg2Cu0.25Fe1O3.75 electrode for YSZ-based potentiometric NH3 sensor. Ceramics International, 2016, 42, 2214-2220.	2.3	27
58	Enhanced pyroelectric properties of leadâ€free BNTâ€BAâ€KNN ceramics for thermal energy harvesting. Journal of the American Ceramic Society, 2019, 102, 3990-3999.	1.9	27
59	Structure, dielectric, ferroelectric, and field-induced strain response properties of (Mg1/3Nb2/3)4+ complex-ion modified Bi0.5(Na0.82K0.18)0.5TiO3 lead-free ceramics. Journal of Alloys and Compounds, 2018, 743, 73-82.	2.8	26
60	Intermediate-temperature conductivity of B-site doped Na0.5Bi0.5TiO3-based lead-free ferroelectric ceramics. Ceramics International, 2016, 42, 16798-16803.	2.3	25
61	Enhanced electrical energy storage properties in La-doped (Bi0.5Na0.5)0.93Ba0.07TiO3 lead-free ceramics by addition of La2O3 and La(NO3)3. Journal of Materials Science, 2017, 52, 10062-10072.	1.7	25
62	Piezoelectric and dielectric aging of Bi0.5(Na0.82K0.18)0.5TiO3 lead-free ferroelectric thick films. Journal of Applied Physics, 2010, 107, .	1.1	24
63	High energy storage performance for dielectric film capacitors by designing 1D SrTiO <sub>3</sub> @SiO <sub>2</sub> nanofillers. Journal of Advanced Dielectrics, 2018, 08, 1850039.	1.5	24
64	Enhanced Pyroelectric and Piezoelectric Figure of Merit of Porous Bi <sub>0.5</sub> (Na <sub>0.82</sub> K <sub>0.18</sub> ) <sub>0.5</sub> TiO <sub>3</sub> Leadâ€Free Ferroelectric Thick Films. Journal of the American Ceramic Society, 2010, 93, 1957-1964.	1.9	23
65	High energy storage density of tetragonal PBLZST antiferroelectric ceramics with enhanced dielectric breakdown strength. Ceramics International, 2020, 46, 3921-3926.	2.3	23
66	The strong electrocaloric effect in molecular ferroelectric ImClO <sub>4</sub> with ultrahigh electrocaloric strength. Journal of Materials Chemistry A, 2020, 8, 16189-16194.	5.2	23
67	High energy density of ferroelectric polymer nanocomposites utilizing PZT@SiO2 nanocubes with morphotropic phase boundary. Chemical Engineering Journal, 2022, 434, 134659.	6.6	23
68	3D printed porous biomass–derived SiCnw/SiC composite for structure–function integrated electromagnetic absorption. Virtual and Physical Prototyping, 2022, 17, 718-733.	5.3	23
69	High remnant polarization, high dielectric constant and impedance performance of Nb/In Co-doped Bi0.49La0.01Na0.49Li0.01TiO3- ceramics. Ceramics International, 2018, 44, 6843-6850.	2.3	22
70	Low-temperature sintered (Na1/2Bi1/2)TiO3-based incipient piezoceramics for co-fired multilayer actuator application. Journal of Materiomics, 2019, 5, 480-488.	2.8	22
71	Enhanced energy storage performance of nanocomposites filled with paraelectric ceramic nanoparticles by weakening the electric field distortion. Ceramics International, 2020, 46, 21149-21155.	2.3	21
72	Significantly improved photocatalytic activity of the SnO2/BiFeO3 heterojunction for pollutant degradation and mechanism. Ceramics International, 2022, 48, 14789-14798.	2.3	21

#	Article	IF	CITATIONS
73	B site doping effect on depinning in Pb(Mn1/3Nb1/3Sb1/3)x(Zr0.825Ti0.175)1–xO3 ferroelectric ceramics. Applied Physics Letters, 2008, 93, 192901.	1.5	20
74	SPS prepared NN-24SBT lead-free relaxor-antiferroelectric ceramics with ultrahigh energy-storage density and efficiency. Scripta Materialia, 2022, 210, 114428.	2.6	19
75	Improved energy storage performance of Ba0.4Sr0.6TiO3 by doping high polarization BiFeO3. Ceramics International, 2021, 47, 14647-14654.	2.3	18
76	Enhanced Electric Field-Induced Strain Properties in Lead-Free BF-BT-Based Piezoceramics by Local Structure Inhomogeneity. ACS Sustainable Chemistry and Engineering, 2022, 10, 1277-1286.	3.2	17
77	Enhanced solar water-splitting performance of TiO2 nanotube arrays by annealing and quenching. Applied Surface Science, 2014, 313, 633-639.	3.1	16
78	Electrical Properties of BST Thin Films Fabricated by a Modified Sol—Gel Processing. Integrated Ferroelectrics, 2005, 70, 1-9.	0.3	15
79	Preparation of poly acrylic acid grafted-mesoporous silica as pH responsive releasing material. Journal of Industrial and Engineering Chemistry, 2014, 20, 2153-2158.	2.9	15
80	The effects of Cu-content on Mg 2 Cu x Fe 1 O 3.5+x electrodes for YSZ-based mixed-potential type NH 3 sensors. Ceramics International, 2016, 42, 9363-9370.	2.3	15
81	Mechanical force-driven growth of elongated BaTiO3 lead-free ferroelectric nanowires. Ceramics International, 2017, 43, 2969-2973.	2.3	15
82	Energy storage performance of sandwich structure composites with strawberry-like Ag@SrTiO3 nanofillers. Chemical Engineering Journal, 2022, 435, 135064.	6.6	15
83	NaNbO <sub>3</sub> â€BaTiO <sub>3</sub> â€NaSbO <sub>3</sub> lead and potassiumâ€free ceramics with thermally stable smallâ€signal piezoelectric properties. Journal of the American Ceramic Society, 2017, 100, 3990-3998.	1.9	14
84	Effect of annealing temperature of a novel Sol–gel process on the electrical properties of low voltage ZnO-based ceramic films. Materials Science and Engineering B: Solid-State Materials for Advanced Technology, 2005, 117, 317-320.	1.7	13
85	High pyroelectric performance due to ferroelectric–antiferroelectric transition near room temperature. Journal of Materials Chemistry C, 2020, 8, 7820-7827.	2.7	13
86	Research Progress on Multilayer‣tructured Polymerâ€Based Dielectric Nanocomposites for Energy Storage. Macromolecular Materials and Engineering, 2022, 307, .	1.7	12
87	Enhanced electrochemical performances with a copper/xylose-based carbon composite electrode. Applied Surface Science, 2018, 436, 639-645.	3.1	11
88	Highly enhanced discharged energy density and superior cyclic stability of Bi0.5Na0.5TiO3-based ceramics by introducing Sr0.7Ca0.3TiO3 component. Materials Chemistry and Physics, 2022, 276, 125402.	2.0	10
89	High energy storage efficiency of NBT-SBT lead-free ferroelectric ceramics. Ceramics International, 2022, 48, 23266-23272.	2.3	10
90	Non-180° domain contributions in Bi0.5(Na0.82K0.18)0.5TiO3 lead-free piezoelectric thick films. Ceramics International, 2015, 41, 10506-10511.	2.3	9

Haibo Zhang

#	Article	IF	CITATIONS
91	Constrained sintering and electrical properties of BNT–BKT lead-free piezoceramic thick films. Ceramics International, 2016, 42, 2534-2541.	2.3	9
92	Enhanced energy storage performance of BNT-ST based ceramics under low electric field via domain engineering. Ceramics International, 2022, 48, 31381-31388.	2.3	9
93	Nonlinear dielectric properties of (Bi0.5Na0.5)TiO3-based lead-free piezoelectric thick films. Applied Physics Letters, 2011, 98, 072908.	1.5	8
94	Enhanced tetragonality and large negative thermal expansion in a new Pb/Bi-based perovskite ferroelectric of (1 â^') Tj ETQq0 0 0 rgBT /Overlock 10 Tf 50 622 Td ( <i>x</i> )PbTiO <sub>3</sub> – <i>x</i> Bi(Z Chemistry Frontiers, 2019, 6, 1990-1995.	n <sub>1/2 3.0</sub>	2V <si< td=""></si<>
95	Phaseâ€Field Study of Electromechanical Coupling in Leadâ€Free Relaxor/Ferroelectric‣ayered Composites. Advanced Electronic Materials, 2019, 5, 1800710.	2.6	8
96	Significantly reduced hysteresis in (Fe1/2Nb1/2)4+-modified 0.75Na1/2Bi1/2TiO3-0.25SrTiO3 lead-free piezoceramics with large strain. Ceramics International, 2021, 47, 17915-17920.	2.3	8
97	Realizing enhanced energy density in ternary polymer blends by intermolecular structure design. Chemical Engineering Journal, 2022, 446, 136980.	6.6	8
98	Preparation and enhanced electric-field-induced strain of textured 91BNT–6BT–3KNN lead-free piezoceramics by TGG method. Journal of Materials Science: Materials in Electronics, 2016, 27, 3076-3081.	1.1	7
99	Tailoring the strain performance of lead-free relaxor/ferroelectric-layered composites. Journal of Electroceramics, 2020, 44, 32-40.	0.8	7
100	Improvement of dielectric properties and energy storage performance in sandwich-structured P(VDF-CTFE) composites with low content of GO nanosheets. Nanotechnology, 2021, 32, 425702.	1.3	7
101	Phase/domain structure and enhanced thermal stable ferro-/pyroelectric properties of (1-x)0.94Na0.48 Bi0.44TiO3-0.06BaTiO3:xZnO ceramics. Journal of the European Ceramic Society, 2020, 40, 699-705.	2.8	6
102	Control of Paste Rheology and Piezoelectric Properties of Bi0.5(Na0.82K0.18)0.5TiO3 Lead-Free Piezoelectric Thick Films Deposited by Screen Printing. International Journal of Applied Ceramic Technology, 2011, 8, 658-668.	1.1	5
103	Effects of Ni addition on the response of La2CuO4 sensing electrode for NO sensor. Sensors and Actuators B: Chemical, 2017, 252, 37-43.	4.0	5
104	FABRICATION AND CHARACTERISTICS OF Pb DOPED BST FERROELECTRIC THIN FILMS FOR UNCOOLED INFRARED FOCAL PLANE ARRAYS. Integrated Ferroelectrics, 2006, 82, 91-99.	0.3	4
105	Composition-sensitive electrical properties of charge nonstoichiometric 0.94Bi0.5+xNa0.5â^'xTiO3–0.06BaTiO3 ceramics. Journal of Advanced Dielectrics, 2019, 09, 1950012.	1.5	4
106	Realizing a ferroelectric state and high pyroelectric performance in antiferroelectric-oxide composites. Dalton Transactions, 2020, 49, 9728-9734.	1.6	4
107	Effect of lithium carbonate on the sintering, microstructure, and functional properties of sol–gelâ€derived Ba0.85Ca0.15Zr0.1Ti0.9O3 piezoceramics. Journal of Materials Research, 2021, 36, 1105-1113.	1.2	3
108	Highâ€energy storage and temperature stable dielectrics properties of leadâ€free BiScO <sub>3</sub> –BaTiO <sub>3</sub> – <i>x</i> (Bi <sub>0.5</sub> Na <sub>0.5</sub> )TiO <sub>3</sub> ceramics. IET Nanodielectrics, 2018, 1, 143-148.	2.0	2

#	Article	IF	CITATIONS
109	Effect of thermal treatment on microstructure and phase of partially-stabilized zirconia. Journal Wuhan University of Technology, Materials Science Edition, 2013, 28, 483-486.	0.4	1
110	Low temperature sintering and microwave dielectric properties of Zr0.3(Zn1/3Nb2/3)0.7TiO4 ceramics doped with CuO-B2O3. Journal of Electroceramics, 2016, 36, 40-45.	0.8	1
111	Fabrication of a Copper/Carbon Composite Based on Biomass for Electrochemical Application. Nihon Enerugi Gakkaishi/Journal of the Japan Institute of Energy, 2017, 96, 273-278.	0.2	1
112	Intermediate-temperature conductivity of Al3+-doped Na0.5Bi0.49TiO3â~'δ lead-free oxide-ion-conductor solid electrolytes. Journal of Materials Science: Materials in Electronics, 2019, 30, 17078-17084.	1.1	1
113	Development of pH-responsive polymer-grafted mesoporous silica. Transactions of the Materials Research Society of Japan, 2013, 38, 597-601.	0.2	1
114	Giant strain and compling effects of relaxor/ferroelectric lead-free composite piezoceramics. , 2015, , .		0
115	Enhanced relaxor behavior and thermal- and frequency-insensitive strain of (Na0.5Bi0.5)0.93Ba0.07Ti1 â~' x(Mn1/3Nb2/3)xO3 ceramics. Journal of Applied Physics, 2020, 127, 194	101 <u>1</u>	0
116	Effect of lithium carbonate on the sintering, microstructure, and functional properties of sol–gel-derived Ba <sub>0.85</sub> Ca <sub>0.15</sub> Zr <sub>0.1</sub> Ti <sub>0.9</sub> O <sub>3</sub> piezoceramics. Journal of Materials Research, 2021, 36, 1-9.	1.2	0